| Bio-information and blood test results | Normal range | Patient II-1 | Patient II-2 |
|---|---|---|---|
| Thyroid stimulating hormone (mIU/l) | 0.34–4.04 | 3.06 | **4.67** |
| Anti-thyroid peroxidase antibody (U/ml) | 0.0–15 | 10 | 10 |
| Anti-thyroglobulin antibody (U/ml) | 0.0–27 | 11 | <10 |
| Thyroglobulin (ng/ml) | 0.0–32.7 | 6.1 | 29.4 |
| Thyroid stimulating hormone receptor antibody (IU/ml) | <1.0 | 0.9 | <1.0 |
| Parathyroid hormone (pg/ml) | 10–65 | 26 | 20 |
| Luteinizing hormone (mIU/ml) | 1.7–8.6 | **13.2** | **9.1** |
| Follicle stimulating hormone (mIU/ml) | 1.5–12.4 | **30.7** | **20.3** |
| Estradiol (pg/ml) | 14.0–43.9 | 18.7 | **10.6** |
| Total testosterone (ng/ml) | 250.0–1100.0 | **90.7** | **53.5** |
| Prolactin (ng/ml) | 4.3–13.7 | 3.7 | 2.5 |
| Cortisol (mg/dl) | 4.0–18.3 | 8.1 | 10.6 |
| Insulin (μU/ml) | 0.0–13.0 | 9.2 | **63.6** |
| Growth hormone (ng/ml) | 0–2.47 | 0.3 | 0.27 |

Bold type indicates values outside the normal range

Table 3. DNA sequence statistics

| Family members | Read length (bp) | Number of reads | Mapping rate (%) | Mean depth (fold) | Coverage (%) |
|---|---|---|---|---|---|
| II-2 (younger brother) | 101 | 47,724,724 | 99.4 | 46.6 | 88.5 |
| II-1 (elder brother) | 101 | 68,584,852 | 99.4 | 59.6 | 86.1 |
| I-1 (father) | 101 | 57,103,807 | 99.3 | 69.3 | 88.5 |
| I-2 (mother) | 101 | 59,776,264 | 99.3 | 56.8 | 86 |
| Average | 101 | 58,297,412 | 99.3 | 58.1 | 87.3 |

or anatomic changes of the retina [14,18,21,40] have been reported. For instance, a study of the pathology of the retina of a 2-year-old girl with AS showed hypocellularity of the ganglionic cell layer, the inner nuclear layer, and the outer nuclear layer (ONL) in addition to an absence of rod and cone outer segments and disruption of retinal pigment epithelium [18,21]; a study of a 42-year-old female with AS revealed severe reduction of all retinal layers containing a complete lack of photoreceptors and deposits of melanin pigments in the inner nuclear layer [14]; and OCT findings of a 5-year-old boy with AS showed only a slight thinning of the central retina [40]. In our patients, OCT findings showed marked retinal thinning (Figure 5A,B). The retinal layers of patient II-2 could not be distinguished because of marked retinal thinning (Figure 5C).

A study using retinal sections of *Alms1* knockout (*Alms1*$^{-/-}$) mice showed loss of the cell bodies in the ONL, shortening of the inner and outer segments, and incorrect localization of rhodopsin to the ONL [7]. The mislocalization of rhodopsin in the *Alms1*$^{-/-}$ mice indicates a defective rhodopsin transport system through the photoreceptor-connecting cilium [7]. The connecting cilium, damaged by loss of function of ALMS1, modifies the outer segments of the photoreceptors. Therefore, it has been suggested that defective protein transport across the connecting cilium is the probable cause of early onset severe retinal degeneration in AS patients [10]. We consider that the marked retinal thinning (Figure 5) and loss of retinal function (Figure 2) observed in our patients are due to a defective transport system across the photoreceptor-connecting cilium, resulting from the homozygous truncated mutation (p.Q2051X).

Variability in the phenotypic expression of AS is observed within sets of affected siblings [14,41–43]. Most patients with AS eventually develop T2DM, although there is wide variability in the age of onset [14]. Here, patient II-1 showed T2DM, but patient II-2 exhibited hyperinsulinemia, a predictor of T2DM (Table 2), suggesting that he might develop T2DM in the future. In addition, patient II-2 showed subclinical hypothyroidism, whereas patient II-1 did not exhibit hypothyroidism (Table 2). Hypothyroidism or subclinical hypothyroidism is reported to exist in approximately 20% of AS patients [14,19]. Most clinical features, such as retinal degeneration, hepatic dysfunction, hyperlipidemia, hypogonadism, short stature, and wide feet, were common features of the affected brothers (Table 1, Table 2); however, slight phenotypic differences in terms of glucose tolerance and thyroid function were observed between them.

ALMS1 protein has several notable sequence features, including an extensive tandem repeat domain (34×47 amino acid approximate tandem repeat, residues 538–2,199), a putative leucine-zipper motif (residues 2,480–2,501), and an ALMS motif (residues 4,035–4,167). Although the precise roles of the above domain and motifs are unknown, it is suggested that two regions of ALMS1—a relatively small internal region (residues 2,261–2,602) and a larger C-terminal region (residues 3,176–4,169)—play important

Table 4. Number of mutations after each filtering step

| Filtering step | Number of mutations |
|---|---|
| 1. Raw single-nucleotide variants plus *insertion–deletion* polymorphisms | 3,506,741 |
| 2. Mutations capable of changing amino acid sequence | 19,574 |
| 3. Mutations filtering by the snpEff score and existing at a frequency of less than 1% in 1000 genomes | 3,685 |
| 4. Mutations filtering by the pattern of inheritance | 17 |
| 5. Mutations expressed in retina, confirmed by SAGE database[a] | 9 |
| 6. Mutations narrowed down using BIOBASE Biologic Database[b] and RetNet database[c] | 1 |

[a]SAGE: serial analysis of gene expression;[b]BIOBASE Biologic Database (EyeSAGE); [c]RetNet database.

roles in targeting ALMS1 to the centrosomes and ciliary basal bodies [44]. In our patients, if the truncated protein caused by the mutation (p.Q2051X) is expressed in the retina, the protein would not contain the two regions important for targeting (residues 2,261–2,602 and residues 3,176–4,169) or the putative leucine-zipper and ALMS motifs. Therefore, this truncated mutation would cause loss of function of ALMS1, resulting in the AS phenotype. Although genotype–phenotype correlations are not clear among AS patients with *ALMS1* mutations [45,46], patients with mutations in exon 8 are reported to have delayed and milder renal complications compared with those with mutations in exons 10 and 16 [13]. In our patients, the p.Q2051X mutation was present in exon 8, explaining normal renal function.

The syndromic disorder AS is often misdiagnosed as LCA, ACHM, or other ciliopathies [11,20,21], so the identification of diagnostic mutations is important. Also, early diagnosis may improve longevity and long-term quality of life. By the whole-exome sequencing analysis technique, we were able to comprehensively determine the disease-causing gene mutation by using the fewest samples possible from the pedigree and analyzing all exon sequences in a relatively short time. Because of the autosomal recessive inheritance pattern, the parents and two affected brothers were enough to narrow down the candidate genes. Consequently, we identified a single causative gene mutation (p.Q2051X of *ALMS1*). Whole-exome sequence analysis should play an important role in future diagnostics for AS.

In conclusion, there has been no report of any AS patient with an *ALMS1* mutation in the Japanese population, probably because AS is an extremely rare inherited disease. We identified a novel *ALMS1* mutation in two brothers of a consanguineous family and examined their clinical features in detail. Our results indicate the presence of different mutations in AS between Japanese and other populations.

## ACKNOWLEGMENTS

We thank the patients and their families for participation in this study. This study was supported by grants to T.I. from the Ministry of Health, Labor and Welfare of Japan (13,803,661), to M.A. and T.H. from the Ministry of Education, Culture, Sports, Science and Technology of Japan (Grant-in-Aid for Scientific Research C, 25,462,744 and 25,462,738), to T.H. from the Vehicle Racing Commemorative Foundation, and to M.F. from the Research Grant for RIKEN Omics Science Center MEXT. The authors wish to acknowledge RIKEN GeNAS for the sequencing of the Exome enriched libraries using the Illumina HiSeq2000.

## REFERENCES

1. Paisey RB, Carey CM, Bower L, Marshall J, Taylor P, Maffei P, Mansell P. Hypertriglyceridaemia in Alström's syndrome: causes and associations in 37 cases. Clin Endocrinol (Oxf) 2004; 60:228-31. [PMID: 14725685].
2. Joy T, Cao H, Black G, Malik R, Charlton-Menys V, Hegele RA, Durrington PN. Alström syndrome (OMIM 203800): a case report and literature review. Orphanet J Rare Dis 2007; 2:49-[PMID: 18154657].
3. Collin GB, Marshall JD, Ikeda A, So WV, Russell-Eggitt I, Maffei P, Beck S, Boerkoel CF, Sicolo N, Martin M, Nishina PM, Naggert JK. Mutations in *ALMS1* cause obesity, type 2 diabetes and neurosensory degeneration in Alström syndrome. Nat Genet 2002; 31:74-8. [PMID: 11941369].
4. Hearn T, Renforth GL, Spalluto C, Hanley NA, Piper K, Brickwood S, White C, Connolly V, Taylor JF, Russell-Eggitt I, Bonneau D, Walker M, Wilson DI. Mutation of *ALMS1*, a large gene with a tandem repeat encoding 47 amino acids, causes Alström syndrome. Nat Genet 2002; 31:79-83. [PMID: 11941370].
5. Hearn T, Spalluto C, Phillips VJ, Renforth GL, Copin N, Hanley NA, Wilson DI. Subcellular localization of ALMS1 supports involvement of centrosome and basal body dysfunction in the pathogenesis of obesity, insulin resistance, and type 2 diabetes. Diabetes 2005; 54:1581-7. [PMID: 15855349].
6. Andersen JS, Wilkinson CJ, Mayor T, Mortensen P, Nigg EA, Mann M. Proteomic characterization of the human centrosome by protein correlation profiling. Nature 2003; 426:570-4. [PMID: 14654843].
7. Collin GB, Cyr E, Bronson R, Marshall JD, Gifford EJ, Hicks W, Murray SA, Zheng QY, Smith RS, Nishina PM, Naggert JK. *Alms1*-disrupted mice recapitulate human Alström syndrome. Hum Mol Genet 2005; 14:2323-33. [PMID: 16000322].
8. Graser S, Stierhof YD, Lavoie SB, Gassner OS, Lamla S, Le Clech M, Nigg EA. Cep164, a novel centriole appendage protein required for primary cilium formation. J Cell Biol 2007; 179:321-30. [PMID: 17954613].
9. Li G, Vega R, Nelms K, Gekakis N, Goodnow C, McNamara P, Wu H, Hong NA, Glynne R. A role for Alström syndrome protein, alms1, in kidney ciliogenesis and cellular quiescence. PLoS Genet 2007; 3:e8-[PMID: 17206865].
10. Adams M, Smith UM, Logan CV, Johnson CA. Recent advances in the molecular pathology, cell biology and genetics of ciliopathies. J Med Genet 2008; 45:257-67. [PMID: 18178628].
11. Badano JL, Mitsuma N, Beales PL, Katsanis N. The ciliopathies: an emerging class of human genetic disorders. Annu Rev Genomics Hum Genet 2006; 7:125-48. [PMID: 16722803].
12. Adams NA, Awadein A, Toma HS. The retinal ciliopathies. Ophthalmic Genet 2007; 28:113-25. [PMID: 17896309].

13. Marshall JD, Hinman EG, Collin GB, Beck S, Cerqueira R, Maffei P, Milan G, Zhang W, Wilson DI, Hearn T, Tavares P, Vettor R, Veronese C, Martin M, So WV, Nishina PM, Naggert JK. Spectrum of *ALMS1* variants and evaluation of genotype-phenotype correlations in Alström syndrome. Hum Mutat 2007; 28:1114-23. [PMID: 17594715].

14. Marshall JD, Bronson RT, Collin GB, Nordstrom AD, Maffei P, Paisey RB, Carey C, Macdermott S, Russell-Eggitt I, Shea SE, Davis J, Beck S, Shatirishvili G, Mihai CM, Hoeltzenbein M, Pozzan GB, Hopkinson I, Sicolo N, Naggert JK, Nishina PM. New Alström syndrome phenotypes based on the evaluation of 182 cases. Arch Intern Med 2005; 165:675-83. [PMID: 15795345].

15. Koç E, Bayrak G, Suher M, Ensari C, Aktas D, Ensari A. Rare case of Alström syndrome without obesity and with short stature, diagnosed in adulthood. Nephrology (Carlton) 2006; 11:81-4. [PMID: 16669965].

16. Akdeniz N, Bilgili SG, Aktar S, Yuca S, Calka O, Kilic A, Kosem M. Alström syndrome with acanthosis nigricans: a case report and literature review. Genet Couns 2011; 22:393-400. [PMID: 22303800].

17. Dyer DS, Wilson ME, Small KW, Pai GS. Alström syndrome: a case misdiagnosed as Bardet-Biedl syndrome. J Pediatr Ophthalmol Strabismus 1994; 31:272-4. [PMID: 7807310].

18. Russell-Eggitt IM, Clayton PT, Coffey R, Kriss A, Taylor DS, Taylor JF. Alström syndrome. Report of 22 cases and literature review. Ophthalmology 1998; 105:1274-80. [PMID: 9663233].

19. Marshall JD, Beck S, Maffei P, Naggert JK. Alström syndrome. Eur J Hum Genet 2007; 15:1193-202. [PMID: 17940554].

20. Lambert SR, Kriss A, Taylor D, Coffey R, Pembrey M. Follow-up and diagnostic reappraisal of 75 patients with Leber's congenital amaurosis. Am J Ophthalmol 1989; 107:624-31. [PMID: 2658617].

21. Russell-Eggitt IM, Taylor DS, Clayton PT, Garner A, Kriss A, Taylor JF. Leber's congenital amaurosis–a new syndrome with a cardiomyopathy. Br J Ophthalmol 1989; 73:250-4. [PMID: 2713302].

22. Ikeda Y, Morita Y, Matsuo Y, Akanuma Y, Itakura H. A case of Alström syndrome associated with situs inversus totalis and characteristic liver cirrhosis. Nippon Naika Gakkai Zasshi 1974; 63:1303-11. [PMID: 4477178].

23. Awazu M, Tanaka T, Sato S, Anzo M, Higuchi M, Yamazaki K, Matsuo N. Hepatic dysfunction in two sibs with Alström syndrome: case report and review of the literature. Am J Med Genet 1997; 69:13-6. [PMID: 9066877].

24. Awazu M, Tanaka T, Yamazaki K, Kato S, Higuchi M, Matsuo N. A 27-year-old woman with Alström syndrome who had liver cirrhosis. Keio J Med 1995; 44:67-73. [PMID: 7658647].

25. Shendure J, Ji H. Next-generation DNA sequencing. Nat Biotechnol 2008; 26:1135-45. [PMID: 18846087].

26. Mardis ER. The impact of next-generation sequencing technology on genetics. Trends Genet 2008; 24:133-41. [PMID: 18262675].

27. Mardis ER. Next-generation DNA sequencing methods. Annu Rev Genomics Hum Genet 2008; 9:387-402. [PMID: 18576944].

28. Ansorge WJ. Next-generation DNA sequencing techniques. New Biotechnol 2009; 25:195-203. [PMID: 19429539].

29. Teer JK, Mullikin JC. Exome sequencing: the sweet spot before whole genomes. Hum Mol Genet 2010; 19:R2R145-51. [PMID: 20705737].

30. Li Y, Vinckenbosch N, Tian G, Huerta-Sanchez E, Jiang T, Jiang H, Albrechtsen A, Andersen G, Cao H, Korneliussen T, Grarup N, Guo Y, Hellman I, Jin X, Li Q, Liu J, Liu X, Sparso T, Tang M, Wu H, Wu R, Yu C, Zheng H, Astrup A, Bolund L, Holmkvist J, Jorgensen T, Kristiansen K, Schmitz O, Schwartz TW, Zhang X, Li R, Yang H, Wang J, Hansen T, Pedersen O, Nielsen R, Wang J. Resequencing of 200 human exomes identifies an excess of low-frequency non-synonymous coding variants. Nat Genet 2010; 42:969-72. [PMID: 20890277].

31. Kim DW, Nam SH, Kim RN, Choi SH, Park HS. Whole human exome capture for high-throughput sequencing. Genome 2010; 53:568-74. [PMID: 20616878].

32. Hodges E, Rooks M, Xuan Z, Bhattacharjee A, Benjamin Gordon D, Brizuela L, Richard McCombie W, Hannon GJ. Hybrid selection of discrete genomic intervals on custom-designed microarrays for massively parallel sequencing. Nat Protoc 2009; 4:960-74. [PMID: 19478811].

33. Takeuchi T, Hayashi T, Bedell M, Zhang K, Yamada H, Tsuneoka H. A novel haplotype with the R345W mutation in the EFEMP1 gene associated with autosomal dominant drusen in a Japanese family. Invest Ophthalmol Vis Sci 2010; 51:1643-50. [PMID: 19850834].

34. Li H, Durbin R. Fast and accurate short read alignment with Burrows-Wheeler transform. Bioinformatics 2009; 25:1754-60. [PMID: 19451168].

35. McKenna A, Hanna M, Banks E, Sivachenko A, Cibulskis K, Kernytsky A, Garimella K, Altshuler D, Gabriel S, Daly M, DePristo MA. The Genome Analysis Toolkit: a MapReduce framework for analyzing next-generation DNA sequencing data. Genome Res 2010; 20:1297-303. [PMID: 20644199].

36. Cingolani P, Platts A. Wang le L, Coon M, Nguyen T, Wang L, Land SJ, Lu X, Ruden DM. A program for annotating and predicting the effects of single nucleotide polymorphisms, SnpEff: SNPs in the genome of Drosophila melanogaster strain w1118; iso-2; iso-3. Fly (Austin) 2012; 6:80-92. [PMID: 22728672].

37. Adzhubei I, Jordan DM, Sunyaev SR. Predicting functional effect of human missense mutations using PolyPhen-2. Curr Protoc Hum Genet 2013; Chapter 7:Unit7 20.

38. Green JS, Parfrey PS, Harnett JD, Farid NR, Cramer BC, Johnson G, Heath O, McManamon PJ, O'Leary E, Pryse-Phillips W. The cardinal manifestations of Bardet-Biedl syndrome, a form of Laurence-Moon-Biedl syndrome. N Engl J Med 1989; 321:1002-9. [PMID: 2779627].

39. Malm E, Ponjavic V, Nishina PM, Naggert JK, Hinman EG, Andreasson S, Marshall JD, Moller C. Full-field electroretinography and marked variability in clinical phenotype of Alström syndrome. Arch Ophthalmol 2008; 126:51-7. [PMID: 18195218].

40. Vingolo EM, Salvatore S, Grenga PL, Maffei P, Milan G, Marshall J. High-resolution spectral domain optical coherence tomography images of Alström syndrome. J Pediatr Ophthalmol Strabismus 2010; 47 Online:e1-3. [PMID: 21158358].

41. Marshall JD, Ludman MD, Shea SE, Salisbury SR, Willi SM, LaRoche RG, Nishina PM. Genealogy, natural history, and phenotype of Alström syndrome in a large Acadian kindred and three additional families. Am J Med Genet 1997; 73:150-61. [PMID: 9409865].

42. Hoffman JD, Jacobson Z, Young TL, Marshall JD, Kaplan P. Familial variable expression of dilated cardiomyopathy in Alström syndrome: a report of four sibs. Am J Med Genet A 2005; 135:96-8. [PMID: 15809999].

43. Hung YJ, Jeng C, Pei D, Chou PI, Wu DA. Alström syndrome in two siblings. J Formos Med Assoc 2001; 100:45-9. [PMID: 11265260].

44. Knorz VJ, Spalluto C, Lessard M, Purvis TL, Adigun FF, Collin GB, Hanley NA, Wilson DI, Hearn T. Centriolar association of ALMS1 and likely centrosomal functions of the ALMS motif-containing proteins C10orf90 and KIAA1731. Mol Biol Cell 2010; 21:3617-29. [PMID: 20844083].

45. Bond J, Flintoff K, Higgins J, Scott S, Bennet C, Parsons J, Mannon J, Jafri H, Rashid Y, Barrow M, Trembath R, Woodruff G, Rossa E, Lynch S, Sheilds J, Newbury-Ecob R, Falconer A, Holland P, Cockburn D, Karbani G, Malik S, Ahmed M, Roberts E, Taylor G, Woods CG. The importance of seeking *ALMS1* mutations in infants with dilated cardiomyopathy. J Med Genet 2005; 42:e10-[PMID: 15689433].

46. Minton JA, Owen KR, Ricketts CJ, Crabtree N, Shaikh G, Ehtisham S, Porter JR, Carey C, Hodge D, Paisey R, Walker M, Barrett TG. Syndromic obesity and diabetes: changes in body composition with age and mutation analysis of *ALMS1* in 12 United Kingdom kindreds with Alström syndrome. J Clin Endocrinol Metab 2006; 91:3110-6. [PMID: 16720663]

Articles are provided courtesy of Emory University and the Zhongshan Ophthalmic Center, Sun Yat-sen University, P.R. China. The print version of this article was created on 24 November 2013. This reflects all typographical corrections and errata to the article through that date. Details of any changes may be found in the online version of the article.

*Molecular Vision* 2013; 19:1580-1590 <http://www.molvis.org/molvis/v19/1580>
Received 1 April 2013 | Accepted 15 July 2013 | Published 20 July 2013



# Molecular characteristics of four Japanese cases with *KCNV2* retinopathy: Report of novel disease-causing variants

**Kaoru Fujinami,[1,2] Kazushige Tsunoda,[1] Natsuko Nakamura,[1] Yu Kato,[1] Toru Noda,[1] Kei Shinoda,[3] Kaoru Tomita,[4] Tetsuhisa Hatase,[5] Tomoaki Usui,[6] Masakazu Akahori,[1] Takeshi Itabashi,[1] Takeshi Iwata,[1] Yoko Ozawa,[2] Kazuo Tsubota,[2] Yozo Miyake[1,7]**

*[1]National Institute of Sensory Organs, National Tokyo Medical Center, Tokyo, Japan; [2]Department of Ophthalmology, Keio University, School of Medicine, Tokyo, Japan; [3]School of Medicine, Teikyo University, Tokyo, Japan; [4]Heiwa Ganka Clinic, Tokyo, Japan; [5]Graduate School of Medical and Dental Sciences, Niigata University, Niigata, Japan; [6]Akiba Eye Clinic, Niigata, Japan; [7]Aichi Medical University, Aichi, Japan*

**Purpose:** To describe the molecular characteristics of four Japanese patients with cone dystrophy with supernormal rod responses (CDSRR).

**Methods:** Four individuals with a clinical and electrophysiological diagnosis of CDSRR were ascertained. The pathognomonic findings of the full-field electroretinograms (ERGs) included a decrease in the rod responses, a square-shaped a-wave, an excessive increase in the b-wave in the bright flash responses, and decreased cone-derived responses. Mutational screening of the coding regions and flanking intronic sequences of the potassium channel, subfamily V, member 2 (*KCNV2*) gene was performed with bidirectional sequencing. The segregation of each allele was confirmed by screening other family members. Subsequent in silico analyses of the mutational consequences for protein function were performed.

**Results:** There were two siblings from one family and one case in each of the two families. One family had a consanguineous marriage. Mutational screening revealed compound heterozygosity for the two alleles, p.C177R and p.G461R, in three patients, and homozygosity for complex alleles, p.R27H and p.R206P, in one patient from the consanguineous family. There were three putative novel variants, p.R27H, p.C177R, and p.R206P. The four variants in the families with *KCNV2* were highly conserved in other species. In silico analyses predicted that all of the missense variants would alter protein function.

**Conclusions:** Biallelic disease-causing variants were identified in four Japanese patients with CDSRR suggesting that the pathognomonic electrophysiological features are helpful in making a molecular diagnosis of *KCNV2*. Three novel variants were identified, and we conclude that there may be a distinct spectrum of *KCNV2* alleles in the Japanese population.

Patients with cone dystrophy and supernormal rod electroretinograms (ERGs) were first reported in 1983, and the abnormality in the ERGs indicated a progressive degeneration of the cone photoreceptors associated with unique rod system abnormalities [1]. More detailed characteristics of this rare, autosomal recessive condition were reported in later studies, and the disease was named cone dystrophy with supernormal rod responses (CDSRR; MIM #610356) [2-8].

Most cases with CDSRR typically present in the first two decades of life with reduced visual acuity, abnormal color vision, and photophobia [8-11]. Night blindness is a later feature of the disorder [8]. The fundus appearance is variable, with some having a normal peripheral retina and a range of macular abnormalities [8-10]. The pattern of the autofluorescence (AF) images is also variable: Young cases have either a normal pattern or small parafoveal ring enhancements, while older cases have a narrow high-signal annulus that can encircle a central atrophic area of the retinal pigment epithelium (RPE) [6,12]. Recently, spectral domain optical coherence tomography (SD-OCT) and adaptive optics scanning laser ophthalmoscope (AOSLO) studies have described morphological changes of the fovea even at the early stages [10,13,14].

The electrophysiological findings are pathognomonic of CDSRR, and they assist in its early diagnosis [3,5,8-12,15-17]. The light-adapted ERGs are usually delayed and decreased in keeping with a generalized cone system dysfunction. There is also a unique rod system abnormality; the dark-adapted ERGs elicited by dim flashes are markedly decreased and delayed, and increasing the flash intensity results in an excessive increase in the b-wave amplitude accompanied by a shortening of the peak time of the b-wave [8,9,11]. A square-shaped a-wave trough of the dark-adapted bright flash ERGs is also a characteristic feature of this disorder [9,11].

Correspondence to: Kazushige Tsunoda, Laboratory of Visual Physiology, National Institute of Sensory Organs, 2-5-1 Higashigaoka, Meguro-ku, Tokyo 152-8902, Japan; Phone: +81334110111; FAX: +81334110185; email: tsunodakazushige@kankakuki.go.jp

CDSRR has been shown to be caused by mutations in the potassium channel, subfamily V, member 2 (*KCNV2*) gene (MIM# 607,604), which encodes a voltage-gated potassium channel subunit, Kv8.2 [18]. This silent subunit is expressed in rod and cone photoreceptors [18-20], and is thought to assemble with other $K^+$ channel subunits such as KCNB1, KCNC1, and KCNF1. These subunits form functional heteromeric channels with altered properties that have a narrowed membrane potential for activation and slow inactivation kinetics [19]. Eventually, these kinetic properties result in transient hyperpolarization overshoots on rapid changes in the inward currents [19]. A deficiency of Kv8.2 by a mutation in *KCNV2* may affect the characteristics of the $I_{kx}$ as first described in amphibian photoreceptors [21]. This deficiency may influence the photoreceptor membrane potential. However, the underlying mechanisms that fully explain the clinical features of CDSRR are still not determined.

More than 50 different disease-causing variants in *KCNV2* have been reported: small insertion and deletion changes or large deletions that constitute a protein truncation and single nucleotide changes with amino acid substitutions [9,10,13,14,16,18,22,23]. Three small case series describe the clinical features of CDSRR in East Asians [3,5,15]; however, molecular genetic studies of these populations have not been published. Thus, the purpose of this study was to determine the molecular genetic characteristics from the clinical and electrophysiological findings of four Japanese patients who were diagnosed with CDSRR.

## METHODS

*Subjects:* Four subjects who were diagnosed with CDSRR from the clinical and electrophysiological findings were ascertained at the National Institute of Sensory Organs, National Tokyo Medical Center, Tokyo, Japan and Niigata University, Niigata, Japan. The natural history of these four patients has been partially reported recently [24]. The procedures used were approved by the ethics committee of each institution, and all procedures were performed in accordance with the principles of the Declaration of Helsinki. Informed consent was obtained from all experimental subjects for all procedures.

*Clinical assessment:* A complete medical history was obtained, and a comprehensive ophthalmological examination was performed on all patients. The photophobia and night blindness episode was obtained on direct questioning. The clinical assessments included measurements of the best-corrected visual acuity (BCVA), dilated ophthalmoscopy, color fundus photography, AF imaging, OCT, and electrophysiological recordings. AF images were obtained with the HRA 2 confocal scanning laser ophthalmoscope (Heidelberg Engineering, Heidelberg, Germany; excitation light, 488 nm; barrier filter, 500 nm; field of view, 30×30°) [25]. The OCT images were obtained with SD-OCT (Cirrus HD-OCT, versions 4.5 and 5.1; Carl Zeiss Meditec, Dublin, CA) [26].

*Electrophysiological assessments:* Full-field ERGs were recorded from the four patients with the minimum standard protocol of the International Society for Clinical Electrophysiology of Vision (ISCEV) [27]. The ERG examination included the following: (i) dark adapted dim flash 0.01 $cd \cdot s \cdot m^{-2}$ (DA 0.01), (ii) dark adapted bright flash 30.0 $cd \cdot s \cdot m^{-2}$ (DA 30.0), (iii) light adapted 3.0 $cd \cdot s \cdot m^{-2}$ at 2 Hz (LA 3.0), and (iv) light adapted 3.0 $cd \cdot s \cdot m^{-2}$ 30 Hz flicker ERG (LA 3.0 30Hz). The extended protocol included the recording of the dark-adapted ERGs elicited by stimulus intensities of 0.001 $cd \cdot s \cdot m^{-2}$, 0.01 $cd \cdot s \cdot m^{-2}$, 0.3 $cd \cdot s \cdot m^{-2}$, 3.0 $cd \cdot s \cdot m^{-2}$, and 30.0 $cd \cdot s \cdot m^{-2}$. Two of the four patients were also recorded with the extended protocol. An excessive or disproportionate increase in the dark adapted b-wave with increasing flash intensity was assessed in these two patients, according to the previous report [9].

*Mutational screening:* After informed consent was obtained, blood samples were collected in EDTA tubes from each subject, and the DNA was extracted with a DNA extraction kit (QIAamp DNA Blood Maxi Kit; Qiagen, Venlo, the Netherlands). All exons and exon–intron boundaries were amplified with polymerase chain reaction (PCR), and the primer sequences used are shown in Table 1. PCR was performed with 20 µl volume containing 0.5 Unit Taq polymerase (PrimeStar GXL DNA polymerase, Takara, Tokyo, Japan). The sequence was determined based on the dideoxy terminator method using an ABI PRISM 3100×l Genetic Analyzer (Applied Biosystems, Foster City, CA) according to the manufacturer's protocol. The SeqScape Software version 2.5 (Applied Biosystems) was used to analyze the sequence alignment. Bidirectional Sanger sequencing was also performed in other family members of the proband, to confirm the segregation of the alleles.

*Molecular genetic analyses:* All of the missense variants identified were analyzed using two software prediction programs, Sorting Intolerant from Tolerance (SIFT) and PolyPhen2 [28,29]. The predicted effects on splicing of all missense variants were assessed with the Human Splicing finder program version 2.4.1. The allele frequency of each variant was estimated with the Exome Variant Server (NHLBI Exome Sequencing Project, Seattle, WA). A multiple sequence alignment program for DNA or proteins, the Clustal Omega, was applied to confirm an evolutionary conservation. Likely non-disease-causing variants (polymorphisms)

Table 1. Primer Sequences and Conditions for KCNV2 Mutational Screening.

| Primer | Sequence (5'–3') | Product size (bp) | PCR annealing (°C) |
|---|---|---|---|
| E1aF | AGGACCTGAGAAGGGGCAGCT | 831 | 71 |
| E1aR | TCCAGGAGGCGGAGGAACTCT | | |
| E1bF | CCCTGCTGTCCACGCTGAATG | 799 | 71 |
| E1bR | CAGCGTGGGTAAGGTGGGTCA | | |
| E1cF | AAGATCCAGCACGAGCTGCGC | 841 | 65 |
| E1cR | ATGGATGTCAAAAGTGGTGGA | | |
| E2aF | AGCTTCTGTTCTTTTCATGAC | 624 | 63 |
| E2aR | GTCTCATAGTTGCTCTGTGTT | | |

bp = base pairs.

were also analyzed with the same protocol applied to likely disease-causing variants.

## RESULTS

The demographic features of the four individuals from three families with CDSRR are summarized in Table 2. There were two siblings (patients 1 and 2) in one family and one case in each of the two families (patients 3 and 4). The pedigree of each family is shown in Figure 1, and a consanguineous marriage was present in family 3.

*Clinical findings:* The age of the patient at the time of the examination was 23, 17, 21, and 17 years with the age of disease onset at 9, 5, 3, and 2 years (Table 2). Three patients complained of photophobia (patients 1, 2, and 4), and all four patients had night blindness. Patient 4 had had mild nystagmus since age 2 years. The decimal BCVA of the four patients ranged from 0.08 to 0.8, and the BCVA of patients 1 and 2 was better than 0.7 in each eye.

The findings obtained from the color fundus photographs, AF images, and SD-OCT images are summarized in Figure 1 and Table 2. The fundus photographs showed mottling of the RPE at the macula in all four patients with subtle patchy granular flecks at the macula in patient 3. A ring enhancement of the AF signal was detected in the AF images of all four patients; three subjects had it centered on the fovea (patients 1, 2, and 3), and one had it at the parafovea (patient 4). In patient 3, the ring enhancement at the fovea was surrounded by patchy granular foci of the high AF signal at the macula.

SD-OCT demonstrated abnormalities in the outer retinal layers in all four patients. The cone outer segment tip line was absent in the macular area in all patients. The photoreceptor inner and outer segment junction line was discontinuous at the fovea in patients 3 and 4, and thinning of the outer retina was detected at the fovea in all four patients.

*Electrophysiological assessments:* The electrophysiological findings are summarized in Table 3, and the ERGs are shown in Figure 2. The full-field ERGs were recorded with the minimum ISCEV standard from patients 2 and 3, and extended protocol full-field ERGs including the dark-adapted ERGs elicited by an intensity series were obtained from patients 1 and 4.

The dark adapted b-wave amplitude elicited by a stimulus intensity 0.01 (DA0.01) was delayed and decreased in patients 3 and 4, but was normal but delayed in patient 1. The responses for DA0.01 were undetectable in patient 2. An excessive increase in the b-wave for the extended protocol was found in two patients, 1 and 4. In addition, the a-wave was square-shaped with a supernormal b-wave elicited by stimulus intensity 30.0 (DA 30.0) in all four patients. The photopic ERGs (LA 3.0 and LA 3.0 30Hz) were decreased in all four patients (Table 3 and Figure 2).

*Molecular genetics:* The molecular genetic findings are summarized in Table 2 and Appendix 1. Likely disease-causing variants in *KCNV2* were identified in all four patients. The four likely disease-causing variants were p.Arg27His, p.Cys177Arg, p.Arg206Pro, and p.Gly461Arg (Appendix 1), and two likely non-disease-causing variants (polymorphisms) were p.Gly61Gly and p.Ala265Ala (Appendix 2). The segregation of each allele was confirmed by screening of other family members for all these variants.

Detailed molecular results including in silico analysis to assist in predicting the pathogenicity of the four disease-causing variants identified are shown in Appendix 1. All of the four likely disease-causing variants were single nucleotide changes with one amino acid substitution (missense), i.e., p.Arg27His, p.Cys177Arg, p.Arg206Pro, and p.Gly461Arg. Compound heterozygosity for the two alleles, p.Cys177Arg and p.Gly461Arg, in patients 1, 2, and 3 and homozygosity for the complex alleles, p.Arg27His and p.Arg206Pro, in patient

Table 2. Summary of demographics, clinical findings and molecular status for four Japanese patients with KCNV2-retinopathy

| Pt, FM, gender | Onset of disease, age at examination (years) | VA | | Fundus | | AF | | OCT | | Mutation status |
|---|---|---|---|---|---|---|---|---|---|---|
| | | RE | LE | RPE mottling | Subtle patchy granular flecks | Ring enhancement | Patchy granular foci of high signal | Absence of COST | Deficit of IS/OS | |
| 1, 1, F | 9, 23 | 0.7 | 0.8 | Macula | ND | Fovea | ND | Fovea | ND | Compund heterozygous [c.529 T>C, p.Cys177Arg]; [c.1381G>A, p.Gly461Arg] |
| 2, 1, M | 5,17 | 0.7 | 0.7 | Macula | ND | Fovea | ND | Fovea | ND | Compund heterozygous [c.529 T>C, p.Cys177Arg]; [c.1381G>A, p.Gly461Arg] |
| 3, 2, F | 3,21 | 0.1 | 0.1 | Macula | Macula | Fovea | Macuala | Macula | Fovea | Compund heterozygous [c.529 T>C, p.Cys177Arg]; [c.1381G>A, p.Gly461Arg] |
| 4, 3, F | 2, 17 | 0.1 | 0.08 | Macula | ND | Para-fovea | ND | Macula | Fovea | Complex homozygous [c.80 G>A, p.Arg27His]; [c.617 G>C, p.Arg206Pro] |

Pt = Patient; FM = family number; VA = logMAR visual acuity; RE = right eye; LE = left eye; RPE = retinal pigment epithelium; AF = autofluorescence; COST = cone outer segment tip line; IS/OS = photoreceptor inner and outer segment junction; ND = not detected. The affected area of each finding is based on the color fundus photographs, AF images, and the OCT images in each column.

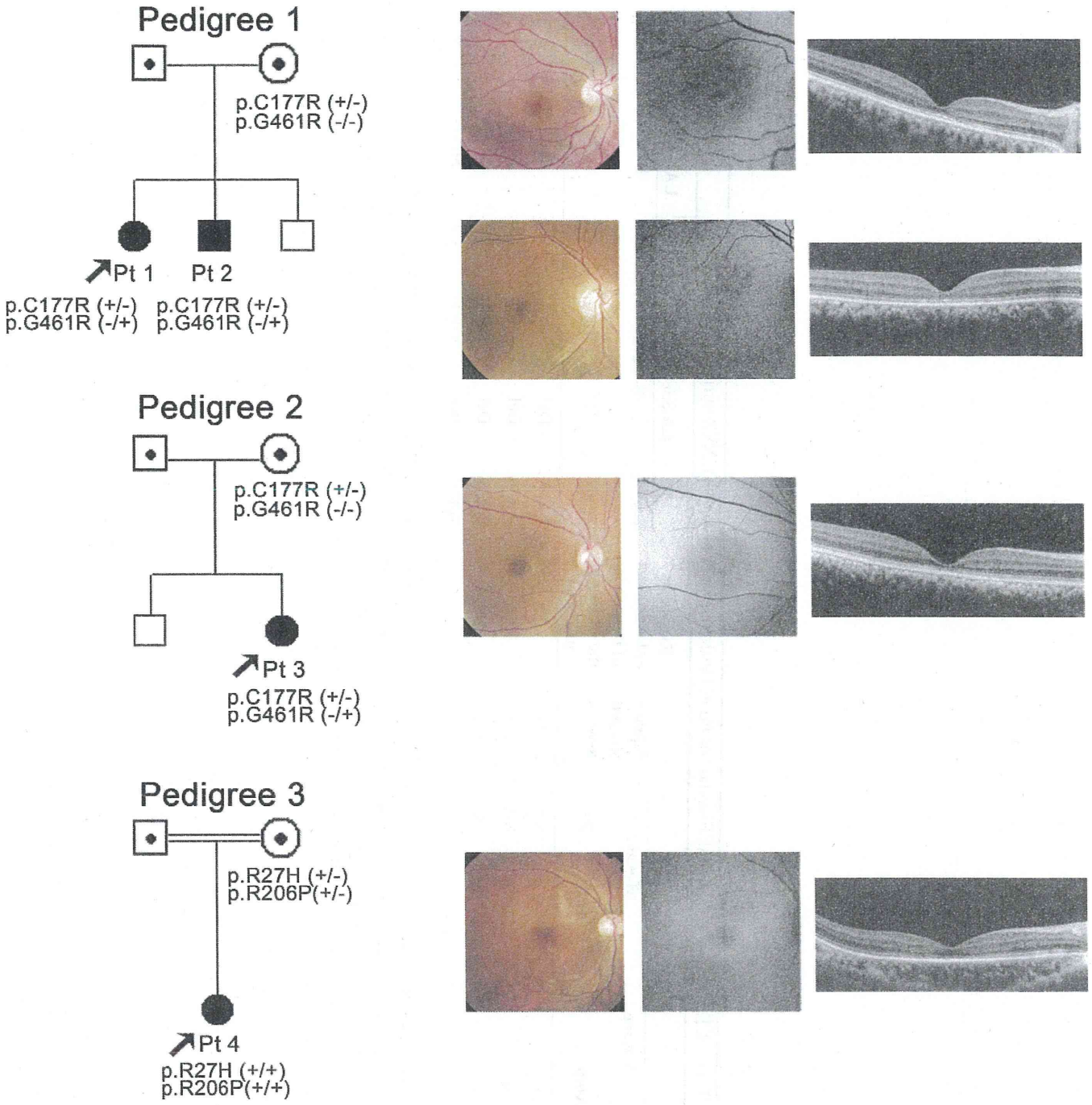


Figure 1. Pedigree and retinal imaging of each patient with potassium channel, subfamily V, member 2 retinopathy. Pedigrees with molecular status of the three families with potassium channel, subfamily V, member 2 (*KCNV2*) retinopathy are shown on the left. Retinal images including color fundus photographs, autofluorescence images, and spectral domain optical coherence tomography are presented on the right. Images of patient 1 (top row), patient 2 (second row from top), patient 3 (third row from top), and patient 4 (bottom row) are shown.

4 were revealed by the segregation analyses. The p.Gly461Arg variant has been reported, and the p.Arg27His, p.Cys177Arg, and p.Arg206Pro variants are putative novel. In silico analysis revealed an "intolerant" protein function or a "probably or possibly damaged" protein but no effect on splicing in the three putative novel variants (SIFT, Poplyphen2, and Human Splicing finder; Appendix 1). The reported missense variant, p.Gly461Arg, with possibly affecting splicing was detected in six out of 13,006 individuals of the Exome Variant Server; the three novel variants, p.Arg27His, p.Cys177Arg, and